

THE XY MODEL ON THE ONE-DIMENSIONAL SUPERLATTICE: STATIC PROPERTIES

J. P. de Lima^a and L. L. Gonçalves^b

^aDepartamento de Física, UFPI, Campus da Ininga, 64049-550
Teresina, Piauí, Brazil.

^bDepartamento de Física, UFCe, Campus do Pici, C.P. 6030, 60451-970
Fortaleza, Ceará, Brazil.

November 15, 2018

Abstract

The XY model ($s = 1/2$) on the one-dimensional alternating superlattice (closed chain) is solved exactly by using a generalized Jordan-Wigner transformation and the Green function method. Closed expressions are obtained for the excitation spectrum, the internal energy, the specific heat, the average magnetization per site, the static susceptibility, χ^{zz} , and the two-spin correlation function in the field direction at arbitrary temperature. At $T = 0$, it is shown that the system presents multiple second order phase transitions induced by the transverse field, which are associated to the zero energy mode with wave number equal to 0 or π . It is also shown that the average magnetization as a function of the field presents, alternately, regions of plateaux (disordered phases) and regions of variable magnetization (ordered phases). The static correlation function presents an oscillating behaviour in the ordered phase and its period goes to infinity at the critical point.

1 Introduction

The experimental development of magnetic superlattices, by using molecular beam epitaxy technique [1-3], has increased the interest in the study of these systems. Although they are three-dimensional systems, there is a predominance of the one-dimensional behaviour in their properties, and this is the main reason for studying one-dimensional superlattices. Therefore, interest has been considerably increased in the study of spin systems on these lattices.

Among the spin systems the XY-model ($s=1/2$), introduced by Lieb et al. [4], occupies a special place, since it can be solved exactly for the homogenous lattice. Although almost all static and dynamical properties are known for the model on the homogeneous lattice (see [5] and references therein), the known results for non-homogeneous periodic one-dimensional systems are restricted to the alternating chain [6-8] and to the excitation spectrum of the general alternating superlattice [9], and its critical behaviour, which has been obtained by using the position space renormalization group approach [10].

In this paper we consider the isotropic XY-model in a transverse field on the one-dimensional alternating superlattice (closed chain). We solve the model by introducing a generalized Jordan-Wigner transformation [9] and by using the Green function equation of motion technique.

In section 2 we determine the relevant Green functions and present a detailed discussion of the excitation spectrum. In section 3 we obtain the internal energy and the specific heat. The induced magnetization is studied in section 4, and in section 5 we calculate the two-spin correlation function. Finally, in section 6, we summarize the results and present the main conclusions.

2 The Excitation Spectrum

The superlattice that we are going to consider consists of cells composed of two subcells A and B with n_A and n_B sites, respectively. The l -th unit cell is shown in Fig. 1. The distance s between two consecutive sites is taken as unity.

If we assume periodic boundary conditions for a chain with N cells, the Hamiltonian of the XY model [4] can be written in the form

$$\begin{aligned}
H = & -\frac{1}{2} \sum_{l=1}^N \left\{ \sum_{m=1}^{n_A-1} J_A S_{l,m}^{A+} S_{l,m+1}^{A-} + \sum_{m=1}^{n_B-1} J_B S_{l,m}^{B+} S_{l,m+1}^{B-} + \right. \\
& + J \left(S_{l,n_A}^{A+} S_{l,1}^{B-} + S_{l,n_B}^{B+} S_{l+1,1}^{A-} \right) + h.c. + \\
& \left. + \sum_{m=1}^{n_A} 2h_A S_{l,m}^{AZ} + \sum_{m=1}^{n_B} 2h_B S_{l,m}^{BZ} \right\} \quad (1)
\end{aligned}$$

where l identifies the cell, $S^\pm = S^x \pm iS^y$, J is the exchange parameter between spins at the interfaces, $J_A(J_B)$ the exchange parameter between spins within the subcell $A(B)$, and $h_A(h_B)$ is the transverse field within the subcell $A(B)$. The spin operators can be expressed in terms of fermion operators using the generalized Jordan-Wigner transformation [9] and, by introducing this transformation, the Hamiltonian can be written in the form

$$\begin{aligned}
H = & -\frac{1}{2} \sum_{l=1}^N \left\{ \sum_{m=1}^{n_A-1} J_A a_{l,m}^\dagger a_{l,m+1} + \sum_{m=1}^{n_B-1} J_B b_{l,m}^\dagger b_{l,m+1} + \right. \\
& + J \left(a_{l,n_A}^\dagger b_{l,1} + b_{l,n_B}^\dagger a_{l+1,1} \right) + h.c. + \\
& \left. + \sum_{m=1}^{n_A} 2h_A \left(a_{l,m}^\dagger a_{l,m} - 1 \right) + \sum_{m=1}^{n_B} 2h_B \left(b_{l,m}^\dagger b_{l,m} - 1 \right) \right\} + \Phi, \quad (2)
\end{aligned}$$

where a 's and b 's are fermion operators, and Φ , given by

$$\Phi = \frac{J}{2} \left(b_{N,n_B}^\dagger a_{1,1} + h.c. \right) \exp \left[i\pi \left(\sum_{l=1}^N \sum_{r=1}^{n_A} a_{l,r}^\dagger a_{l,r} + \sum_{l=1}^N \sum_{r=1}^{n_B} b_{l,r}^\dagger b_{l,r} \right) \right], \quad (3)$$

is a boundary term which will be neglected. As it has been shown [11], this boundary term, in the

thermodynamic limit, does not affect the excitation spectrum, the static properties of the system nor the dynamic correlation function in the field direction. Introducing the Fourier transforms [9],

$$a_{Qk_1} = \sqrt{\frac{2}{N(n_A+1)}} \sum_{l,m} \exp(iQdl) \sin(mk_1) a_{l,m}, \quad (4)$$

$$b_{Qk_2} = \sqrt{\frac{2}{N(n_B+1)}} \sum_{l,m} \exp(iQdl) \sin(mk_2) b_{l,m}, \quad (5)$$

where $k_1 = n_1\pi/(n_A+1)$, $n_1 = 1, 2, \dots, n_A$, $k_2 = n_2\pi/(n_B+1)$, $n_2 = 1, 2, \dots, n_B$, $Q = 2\pi n/N$, $n = 1, 2, \dots, N$, $d = n_A + n_B$ is the size of the cell, the Hamiltonian can be written as

$$H = \sum_Q H_Q + N \left(\frac{n_A h_A + n_B h_B}{2} \right) \quad (6)$$

where H_Q is given by

$$\begin{aligned} H_Q &= \sum_{k_1} E_{k_1}^A a_{Qk_1}^\dagger a_{Qk_1} + \sum_{k_2} E_{k_2}^B b_{Qk_2}^\dagger b_{Qk_2} + \\ &- \frac{J}{\sqrt{(n_A+1)(n_B+1)}} \sum_{k_1, k_2} \{ [\sin(k_1 n_A) \sin k_2 \\ &+ \sin(k_2 n_B) \sin k_1 \exp(iQd) a_{Qk_1}^\dagger b_{Qk_2}] + h.c. \}, \end{aligned} \quad (7)$$

with $E_{k_1(2)}^{A(B)} = -J_{A(B)} \cos k_1(2) - h_{A(B)}$.

As in the study of the excitation spectrum [9] we will solve the model by using the Green function method [12]. Adopting the notation $\langle\langle \mathfrak{R}_1(t); \mathfrak{R}_2(0) \rangle\rangle_r$ for the retarded anticommutator function, where \mathfrak{R}_1 and \mathfrak{R}_2 are arbitrary operators, and introducing the time Fourier transform defined as

$$\langle\langle \mathfrak{R}_1(t); \mathfrak{R}_2(0) \rangle\rangle_r = \frac{1}{2\pi} \int_{-\infty}^{\infty} \langle\langle \mathfrak{R}_1; \mathfrak{R}_2 \rangle\rangle \exp(-i\omega t) d\omega, \quad (8)$$

we can write the equation of motion for the Green function $\langle\langle a_{Qk_1}; a_{Q'k'_1}^\dagger \rangle\rangle$ in the form [12]

$$\begin{aligned} \langle\langle a_{Qk_1}; a_{Q'k'_1}^\dagger \rangle\rangle &= \delta_{k_1 k'_1} (\omega - E_{k_1}^A)^{-1} + \\ &- \frac{J (\omega - E_{k_1}^A)^{-1}}{\sqrt{(n_A+1)(n_B+1)}} \sum_{k_2} [\sin k_2 \sin(n_A k_1) + \\ &+ (iQd) \sin k_1 \sin(n_B k_2)] \langle\langle b_{Qk_2}; a_{Q'k'_1}^\dagger \rangle\rangle, \end{aligned} \quad (9)$$

where we have assumed $\hbar = 1$.

Likewise we can write for $\ll b_{Qk_2}; a_{Q'k_1}^\dagger \gg$ the result

$$\begin{aligned} \langle\langle b_{Qk_2}; a_{Q'k_1}^\dagger \rangle\rangle &= -\frac{J(\omega - E_{k_2}^B)^{-1}}{\sqrt{(n_A + 1)(n_B + 1)}} \sum_{k_1'} [\sin k_2 \sin(n_A k_1') + \\ &+ \exp(-iQd) \sin k_1' \sin(n_B k_2)] \langle\langle a_{Qk_1'}; a_{Q'k_1}^\dagger \rangle\rangle. \end{aligned} \quad (10)$$

Eqs. (11) and (12) constitute a closed set which can be easily solved by introducing the operators $A_{Q,n}$ and $B_{Q,n}$ defined by

$$A_{Q,n} = \sqrt{\frac{2}{n_A + 1}} \sum_{k_1} \sin(nk_1) a_{Qk_1}, \quad (11)$$

$$B_{Q,n} = \sqrt{\frac{2}{n_B + 1}} \sum_{k_2} \sin(nk_2) b_{Qk_2} \quad (12)$$

Therefore by eliminating the function $\ll b_{Qk_2}; a_{Q'k_1}^\dagger \gg$ from eqs.(11) and (12) and introducing the operator $A_{Q,n}$ we can find the result

$$\begin{aligned} \langle\langle A_{Q,m}; A_{Q',n}^\dagger \rangle\rangle &= \frac{2}{J} \sqrt{\frac{n_B + 1}{n_A + 1}} f_{m,n}^A(\omega) \delta_{Q,Q'} + \\ &+ [f_{1,1}^B(\omega) f_{m,n_A}^A(\omega) + \exp(iQd) f_{1,n_B}^B(\omega) f_{m,1}^A(\omega)] \langle\langle A_{Q,n_A}; A_{Q',n}^\dagger \rangle\rangle + \\ &+ [f_{1,1}^B(\omega) f_{m,1}^A(\omega) + \exp(-iQd) f_{1,n_B}^B(\omega) f_{m,n_A}^A(\omega)] \langle\langle A_{Q,1}; A_{Q',n}^\dagger \rangle\rangle \end{aligned} \quad (13)$$

where

$$f_{m,n}^A(\omega) \equiv \frac{J}{\sqrt{(n_A + 1)(n_B + 1)}} \sum_{k_1} \frac{\sin(mk_1) \sin(nk_1)}{\omega - E_{k_1}^A}, \quad (14)$$

$$f_{m,n}^B(\omega) \equiv \frac{J}{\sqrt{(n_A + 1)(n_B + 1)}} \sum_{k_2} \frac{\sin(mk_2) \sin(nk_2)}{\omega - E_{k_2}^B}. \quad (15)$$

From eq. (15) we can find immediately that $\ll A_{Q,m}; A_{Q',n}^\dagger \gg$ is given by

$$\begin{aligned}
\langle\langle A_{Q,m}; A_{Q',n}^\dagger \rangle\rangle &= \frac{2}{J} \sqrt{\frac{n_B+1}{n_A+1}} \delta_{Q,Q'} \left\{ f_{m,n}^A(\omega) + \frac{1}{R_Q(\omega)} \times \right. \\
&\times \left\{ [f_{1,1}^B(\omega) f_{m,n_A}^A(\omega) + \exp(iQd) f_{1,n_B}^B(\omega) f_{m,1}^A(\omega)] \times \right. \\
&\times [f_{1,n}^A(\omega) (f_{1,n_A}^A(\omega) f_{1,1}^B(\omega) + f_{1,1}^A(\omega) f_{1,n_B}^B(\omega) \exp(-iQd)) + \\
&+ f_{n,n_A}^A(\omega) (1 - f_{1,1}^A(\omega) f_{1,1}^B(\omega) - f_{1,n_A}^A(\omega) f_{1,n_B}^B(\omega) \exp(-iQd))] + \\
&+ [f_{1,1}^B(\omega) f_{m,1}^A(\omega) + \exp(-iQd) f_{1,n_B}^B(\omega) f_{m,n_A}^A(\omega)] \times \\
&\times [f_{n,n_A}^A(\omega) (f_{1,n_A}^A(\omega) f_{1,1}^B(\omega) + f_{1,1}^A(\omega) f_{1,n_B}^B(\omega) \exp(iQd)) + \\
&+ f_{1,n}^A(\omega) (1 - f_{1,1}^A(\omega) f_{1,1}^B(\omega) - f_{1,n_A}^A(\omega) f_{1,n_B}^B(\omega) \exp(iQd))] \left. \left. \right\} \right\}. \tag{16}
\end{aligned}$$

The details of the calculation can be found in ref. [13].

By a similar procedure we can write the set of equations

$$\begin{aligned}
\langle\langle b_{Qk_2}; b_{Q'k'_2}^\dagger \rangle\rangle &= \delta_{k_2k'_2} (\omega - E_{k_2}^B)^{-1} + \\
&- \frac{J (\omega - E_{k_2}^B)^{-1}}{\sqrt{(n_A+1)(n_B+1)}} \sum_{k_1} [\sin k_2 \sin(n_A k_1) + \\
&+ \exp(-iQd) \sin k_1 \sin(n_B k_2)] \langle\langle a_{Qk_1}; b_{Q'k'_2}^\dagger \rangle\rangle, \tag{17}
\end{aligned}$$

$$\begin{aligned}
\langle\langle a_{Qk_1}; b_{Q'k'_2}^\dagger \rangle\rangle &= - \frac{J (\omega - E_{k_1}^A)^{-1}}{\sqrt{(n_A+1)(n_B+1)}} \sum_{k_2} [\sin k_2 \sin(n_A k_1) + \\
&+ \exp(iQd) \sin k_1 \sin(n_B k_2)] \langle\langle b_{Qk_2}; b_{Q'k'_2}^\dagger \rangle\rangle, \tag{18}
\end{aligned}$$

which can be solved by eliminating the function $\ll a_{Qk_1}; b_{Q'k'_2}^\dagger \gg$ in the previous equation and by

introducing the operator $B_{Q,n}$. This procedure leads to the set of equations

$$\begin{aligned}
\langle\langle B_{Q,m}; B_{Q',n}^\dagger \rangle\rangle &= \frac{2}{J} \sqrt{\frac{n_A+1}{n_B+1}} f_{m,n}^B(\omega) \delta_{Q,Q'} + \\
&+ [f_{1,1}^A(\omega) f_{m,n_B}^B(\omega) + \exp(iQd) f_{1,n_A}^A(\omega) f_{m,1}^B(\omega)] \langle\langle B_{Q,n_B}; B_{Q',n}^\dagger \rangle\rangle + \\
&+ [f_{1,1}^A(\omega) f_{m,1}^B(\omega) + \exp(-iQd) f_{1,n_A}^A(\omega) f_{m,n_B}^B(\omega)] \langle\langle B_{Q,1}; B_{Q',n}^\dagger \rangle\rangle,
\end{aligned} \tag{19}$$

and, as we can see, it can be obtained from eq. (15), provided we make the substitution $A \rightarrow B$ and $B \rightarrow A$. Therefore $\langle\langle B_{Q,m}; B_{Q',n}^\dagger \rangle\rangle$ is obtained from eq. (18) by introducing the previous transformation.

The excitation spectrum is given by the poles of $\langle\langle A_{Q,m}; A_{Q',n}^\dagger \rangle\rangle$, or $\langle\langle B_{Q,m}; B_{Q',n}^\dagger \rangle\rangle$, and corresponds to the solution of the equation $R_Q(\omega) = 0$, which is explicitly given by [9]

$$\begin{aligned}
1 - 2f_{1,n_A}^A(\omega) f_{1,n_B}^B(\omega) \cos(Qd) - 2f_{1,1}^A(\omega) f_{1,1}^B(\omega) + \\
+ [(f_{1,1}^A(\omega))^2 - (f_{1,n_A}^A(\omega))^2] [(f_{1,1}^B(\omega))^2 - (f_{1,n_B}^B(\omega))^2] = 0.
\end{aligned} \tag{20}$$

As mentioned in our previous paper [9], it should be noted that the values $\omega = E_{k_1}^A$ and $\omega = E_{k_2}^B$ are not poles of $\langle\langle A_{Q,m}; A_{Q',n}^\dagger \rangle\rangle$, since in this limit the function is finite. Therefore, as expected, the spectrum of each subcell does not coincide with spectrum of the superlattice, and contains $n_A + n_B$ branches [9].

The general solution of this equation is determined numerically, although analytical solutions can be found for some special cases. For instance for $n_A = n_B = 2, h_A = h_B = h$, we can express explicitly the solution in the form

$$\omega_Q = -h \pm \frac{1}{\sqrt{2}} \sqrt{c \pm \sqrt{g(Qd)}}, \tag{21}$$

where

$$c \equiv \frac{J^2}{2} + \frac{1}{4} (J_A^2 + J_B^2), \tag{22}$$

$$g(Qd) \equiv \frac{1}{2} J^2 J_A J_B \cos(Qd) + \frac{J^2}{4} (J_A^2 + J_B^2) + \frac{1}{16} (J_A^2 - J_B^2)^2, \tag{23}$$

which for $J_A = J_B$ reproduces the known results [6,7].

In the homogeneous medium limit, the spectrum obtained from the eq. (22) presents $n_A + n_B$ branches, which correspond to a $(n_A + n_B - 1)$ -folding of the spectrum. As an example of this limit we present in Fig. 2 the excitation spectrum for $n_A = 2, n_B = 3, J_A = J_B = J = 1$ and $h_A = h_B = 2$.

For zero field and $n_A + n_B$ odd, there is a zero energy mode with wave number different from zero, as shown in Fig. 3 for $n_A = 2, n_B = 3, J_A = 2, J_B = 3$ and $J = 1$. On the other hand,

for $n_A + n_B$ even this mode is not present, and for each wave number Q there are symmetrical solutions $+\omega_Q$ and $-\omega_Q$, as can be seen in Fig. 4 for $n_A = n_B = 4$, $J_A = 0.3$, $J_B = 3$ and $J = 1$.

As it has already been shown [14], the effect of a homogeneous field, $h_A = h_B = h$, is to shift the zero field spectrum. This can also be shown directly from eq. (22) and, consequently, the existence of a mode of zero energy will depend on the strength of the field.

As we can also see in Fig. 4, the extreme bands of the spectrum are very narrow, and this is related to the difference between the exchange parameters of subcells A and B . As the difference between the parameters of the media A and B decreases, the dispersion increases, and the gaps tend to zero. This is the expected behaviour, since we have a maximum dispersion in the homogeneous limit, as shown in Fig. 2. In all cases presented the number of branches is equal to the number of sites per cell.

Again, we note that the spectrum can also be calculated exactly by using the position space renormalization group approach [10], and approximately by using a transfer matrix method [15]. Although the latter is an approximate method, we have shown that it reproduces numerically the exact result [5,8].

3 The Internal Energy and the Specific Heat

The operator H_Q defined in eq. (9) can be written in terms of operators $A_{Q,n}$ and $B_{Q,n}$ in the form

$$\begin{aligned}
H_Q &= \frac{2}{n_A + 1} \sum_{k_1} E_{k_1}^A \left[\sum_{n=1}^{n_A} \sin(nk_1) A_{Q,n}^\dagger \right] \left[\sum_{n=1}^{n_A} \sin(nk_1) A_{Q,n} \right] + \\
&+ \frac{2}{n_B + 1} \sum_{k_2} E_{k_2}^B \left[\sum_{n=1}^{n_B} \sin(nk_2) B_{Q,n}^\dagger \right] \left[\sum_{n=1}^{n_B} \sin(nk_2) B_{Q,n} \right] + \\
&- \frac{J}{2} \left[A_{Q,n_A}^\dagger B_{Q,1} + \exp(iQd) A_{Q,1}^\dagger B_{Q,n_B} + h.c. \right].
\end{aligned} \tag{24}$$

From this equation we can see that the internal energy, $\langle H \rangle = \sum_Q \langle H_Q \rangle$, can be calculated from the Green function $G_Q(\omega)$ given by

$$G_Q(\omega) = G1_Q(\omega) + G2_Q(\omega) + G3_Q(\omega), \tag{25}$$

where

$$G1_Q(\omega) = \frac{2}{n_A + 1} \sum_{k_1} E_{k_1}^A \left[\sum_{m=1}^{n_A} \sum_{n=1}^{n_A} \sin(mk_1) \sin(nk_1) \langle\langle A_{Q,m}; A_{Q,n}^\dagger \rangle\rangle \right] \quad (26)$$

$$G2_Q(\omega) = \frac{2}{n_B + 1} \sum_{k_2} E_{k_2}^B \left[\sum_{m=1}^{n_B} \sum_{n=1}^{n_B} \sin(mk_2) \sin(nk_2) \langle\langle B_{Q,m}; B_{Q,n}^\dagger \rangle\rangle \right] \quad (27)$$

$$G3_Q(\omega) = -\frac{J}{2} \left[\langle\langle B_{Q1}; A_{Q,n_A}^\dagger \rangle\rangle + \exp(iQd) \langle\langle B_{Qn_B}; A_{Q,1}^\dagger \rangle\rangle + \langle\langle A_{Qn_A}; B_{Q,1}^\dagger \rangle\rangle + \exp(-iQd) \langle\langle A_{Q1}; B_{Q,n_B}^\dagger \rangle\rangle \right]. \quad (28)$$

The Green functions $\langle\langle B_{Q1}; A_{Q,n_A}^\dagger \rangle\rangle$, $\langle\langle B_{Qn_B}; A_{Q,1}^\dagger \rangle\rangle$, $\langle\langle A_{Qn_A}; B_{Q,1}^\dagger \rangle\rangle$ and $\langle\langle A_{Q1}; B_{Q,n_B}^\dagger \rangle\rangle$ can, with the aid of eqs. (11-14) and (19,20), be written in terms of the functions $\langle\langle A_{Q,m}; A_{Q',n}^\dagger \rangle\rangle$ and $\langle\langle B_{Q,m}; B_{Q',n}^\dagger \rangle\rangle$, and are given by

$$\begin{aligned} \langle\langle A_{Q,1}; B_{Q',n_B}^\dagger \rangle\rangle &= -\sqrt{\frac{n_B + 1}{n_A + 1}} \left[f_{1,n_A}^A(\omega) \langle\langle B_{Q,1}; B_{Q',n_B}^\dagger \rangle\rangle + \right. \\ &\quad \left. + \exp(iQd) f_{1,1}^A(\omega) \langle\langle B_{Q,n_B}; B_{Q',n_B}^\dagger \rangle\rangle \right], \end{aligned} \quad (29)$$

$$\begin{aligned} \langle\langle A_{Q,n_A}; B_{Q',1}^\dagger \rangle\rangle &= -\sqrt{\frac{n_B + 1}{n_A + 1}} \left[f_{1,1}^A(\omega) \langle\langle B_{Q,1}; B_{Q',1}^\dagger \rangle\rangle + \right. \\ &\quad \left. + \exp(iQd) f_{1,n_A}^A(\omega) \langle\langle B_{Q,n_B}; B_{Q',1}^\dagger \rangle\rangle \right], \end{aligned} \quad (30)$$

$$\begin{aligned} \langle\langle B_{Q,n_B}; A_{Q',1}^\dagger \rangle\rangle &= -\sqrt{\frac{n_A + 1}{n_B + 1}} \left[f_{1,n_B}^B(\omega) \langle\langle A_{Q,n_A}; A_{Q',1}^\dagger \rangle\rangle + \right. \\ &\quad \left. + \exp(-iQd) f_{1,1}^B(\omega) \langle\langle A_{Q,1}; A_{Q',1}^\dagger \rangle\rangle \right], \end{aligned} \quad (31)$$

$$\begin{aligned} \langle\langle B_{Q1}; A_{Q',n_A}^\dagger \rangle\rangle &= -\sqrt{\frac{n_A + 1}{n_B + 1}} \left[f_{1,1}^B(\omega) \langle\langle A_{Q,n_A}; A_{Q',n_A}^\dagger \rangle\rangle + \right. \\ &\quad \left. + \exp(-iQd) f_{1,n_B}^B(\omega) \langle\langle A_{Q,1}; A_{Q',n_A}^\dagger \rangle\rangle \right]. \end{aligned} \quad (32)$$

Then by using eqs. (18), and (31-34) in eqs. (28-29) we obtain the Green functions, $G1_Q(\omega)$,

$G2_Q(\omega)$ and $G3_Q(\omega)$, which are given by [13]

$$\begin{aligned}
G1_Q(\omega) &= \sum_{k_1} \frac{E_{k_1}^A}{(\omega - E_{k_1}^A)} + \frac{J\bar{c}}{R_Q(\omega)} \sum_{k_1} \frac{E_{k_1}^A}{(\omega - E_{k_1}^A)^2} \\
&\times \left\{ \sin^2 k_1 \left[f_{1,1}^B(\omega) - f_{1,1}^A(\omega) \left((f_{1,1}^B(\omega))^2 - (f_{1,n_B}^B(\omega))^2 \right) \right] + \right. \\
&+ \sin k_1 \sin(n_A k_1) \left[f_{1,n_B}^B(\omega) \cos(Qd) + \right. \\
&\left. \left. + f_{1,n_A}^A(\omega) \left((f_{1,1}^B(\omega))^2 - (f_{1,n_B}^B(\omega))^2 \right) \right] \right\}, \tag{33}
\end{aligned}$$

$$\begin{aligned}
G3_Q(\omega) &= \frac{2}{R_Q(\omega)} \left\{ 1 - R_Q(\omega) - \left[(f_{1,1}^A(\omega))^2 - (f_{1,n_A}^A(\omega))^2 \right] \right. \\
&\times \left. \left[(f_{1,1}^B(\omega))^2 - (f_{1,n_B}^B(\omega))^2 \right] \right\}, \tag{34}
\end{aligned}$$

and $G2_Q(\omega)$ can be obtained from $G1_Q(\omega)$ by introducing the transformations $k_1 \rightarrow k_2$, $A \rightarrow B$ and $B \rightarrow A$. From these results we can show that the expression for $G_Q(\omega)$ has the form

$$G_Q(\omega) = \frac{1}{R_Q(\omega)} \left[\mathcal{G}(f_{1,1}^A(\omega), f_{1,n_A}^A(\omega), f_{1,1}^B(\omega), f_{1,n_B}^B(\omega)) \right]. \tag{35}$$

Then, the internal energy, $\langle H \rangle = \sum_Q \langle H_Q \rangle$, can be obtained from the expression [7]

$$\langle H \rangle = \frac{1}{\pi} \sum_Q \int_{-\infty}^{\infty} \frac{Im(G_Q(\omega))}{e^{\beta\omega} + 1} d\omega, \tag{36}$$

where, as usual, $\beta = 1/k_B T$.

By using the Dirac identity

$$\frac{1}{x - x_0 \pm i\varepsilon} \equiv \mathcal{P} \left(\frac{1}{x - x_0} \right) \mp i\pi\delta(x - x_0), \tag{37}$$

we can show immediately that $Im(G_Q(\omega))$ can be written in the form

$$Im(G_Q(\omega)) = \sum_r F_{Q,r} \delta(\omega - \omega_{Q,r}), \tag{38}$$

where

$$F_{Q,r} = \frac{R_Q(\omega_{Q,r}) G_Q(\omega_{Q,r})}{R'_Q(\omega_{Q,r})}, \tag{39}$$

where r labels the branches of the spectrum and $R'_Q(\omega)$ is equal to $dR_Q(\omega)/d\omega$.

The specific heat is obtained from eq. (38) and can be written in the form

$$C = \frac{1}{N} \frac{d\langle H \rangle}{dT} = \frac{k_B \beta^2}{N\pi} \sum_Q \int_{-\infty}^{\infty} \frac{\omega e^{\beta\omega} \text{Im}(G_Q(\omega))}{(e^{\beta\omega} + 1)^2} d\omega. \quad (40)$$

The behaviour of the internal energy as a function of temperature does not present any remarkable difference as we change the superlattice parameters. A typical result is shown in Fig. 5 where the internal energy is shown as a function of temperature T^* ($T^* \equiv k_B T$) for $n_A = n_B = 10$, $J_A = 2$, $J_B = 3$, $J = 1$, $h_A = h_B = 1.5$.

On the other hand, the behaviour of the specific heat as a function of temperature is very susceptible to these parameters. It can present a single peak or a double peak, as it can be seen in Figs. 6 and 7. This important feature, namely, the appearance of the double peak, is a consequence of the packing of the branches of the excitation spectrum, which is strongly dependent on the interaction parameters. As we increase the field, we move the spectrum downwards and this has the effect of suppressing one peak of the specific heat. This is shown in Fig. 8, where we have used the same lattice parameters of Fig. 7, and a larger field.

In Figs. 9 and 10 we present the low temperature behaviour of the specific heat shown in Figs. 7 and 8, respectively. For the results shown in Fig. 9, the excitation spectrum has a zero energy mode contrary to the case shown in Fig. 10, where it is not present, as can be verified by using the analytical solution presented in eq. (23). As expected, the derivative of the specific heat, dC/dT^* , at $T = 0$, is equal to zero only when there is a zero mode energy in the spectrum.

4 The Induced Magnetization and the Susceptibility χ^{zz}

The local induced magnetization which corresponds to the average value of $S_{j,m}^{A^z}$ and $S_{j,m}^{B^z}$, is given by

$$\langle S_{j,m}^{A^z} \rangle = \langle a_{j,m}^\dagger a_{j,m} \rangle - \frac{1}{2} \quad \text{and} \quad \langle S_{j,m}^{B^z} \rangle = \langle b_{j,m}^\dagger b_{j,m} \rangle - \frac{1}{2}, \quad (41)$$

which can be determined from the Green functions $\ll a_{j,m}; a_{j,m}^\dagger \gg$ and $\ll b_{j,m}; b_{j,m}^\dagger \gg$, respectively. In terms of the operators $A_{Q,m}$ and $B_{Q,m}$ these functions can be written in the form

$$\langle\langle a_{j,m}; a_{j,m}^\dagger \rangle\rangle = \frac{1}{N} \sum_{Q,Q'} \exp[-i(Q - Q')d] \langle\langle A_{Q,m}; A_{Q',m}^\dagger \rangle\rangle \quad (42)$$

and

$$\langle\langle b_{j,m}; b_{j,m}^\dagger \rangle\rangle = \frac{1}{N} \sum_{Q,Q'} \exp[-i(Q - Q')d] \langle\langle B_{Q,m}; B_{Q',m}^\dagger \rangle\rangle. \quad (43)$$

Then introducing in eq. (44) the function $\ll A_{Q,m}; A_{Q',m}^\dagger \gg$, which is given in eq. (18), we can write $\ll a_{j,m}; a_{j,m}^\dagger \gg$ in the form

$$\begin{aligned}
\langle\langle a_{j,m}; a_{j,m}^\dagger \rangle\rangle &= \frac{2}{NJ} \sqrt{\frac{n_B+1}{n_A+1}} \sum_Q \{ f_{m,m}^A(\omega) + \\
&+ \frac{1}{R_Q(\omega)} [f_{1,m}^A(\omega) f_{m,n_A}^A(\omega) (2f_{1,n_B}^B(\omega) \cos(Qd) + 2f_{1,n_A}^A(\omega) \\
&\times ((f_{1,1}^B(\omega))^2 - (f_{1,n_B}^B(\omega))^2)) + ((f_{1,m}^A(\omega))^2 - (f_{m,n_A}^A(\omega))^2) \\
&\times (f_{1,1}^B(\omega) + f_{1,1}^A(\omega)) ((f_{1,1}^B(\omega))^2 - (f_{1,n_B}^B(\omega))^2)] \}. \quad (44)
\end{aligned}$$

The function $\ll b_{j,m}; b_{j,m}^\dagger \gg$ is obtained from $\ll a_{j,m}; a_{j,m}^\dagger \gg$ by introducing the transformations $f^A \rightarrow f^B$, $f^B \rightarrow f^A$, $n_A \rightarrow n_B$ and $n_B \rightarrow n_A$. From this result we can write

$$\langle a_{j,m}^\dagger a_{j,m} \rangle = \frac{1}{\pi} \int_{-\infty}^{\infty} \frac{Im \left(\langle\langle a_{j,m}; a_{j,m}^\dagger \rangle\rangle \right)}{e^{\beta\omega} + 1} d\omega, \quad (45)$$

which, in the thermodynamic limit, allows us to obtain $\langle S_{j,m}^{A^z} \rangle$ from the equation

$$\langle S_{j,m}^{A^z} \rangle = -\frac{1}{2} + \frac{1}{2\pi} \sum_r \int_0^{2\pi} \frac{F(q, \omega_{q,r}, h)}{(e^{\beta\omega_{q,r}} + 1) \frac{dR_Q(\omega)}{d\omega} |_{\omega_{q,r}}} dq, \quad (46)$$

where

$$\begin{aligned}
F(q, \omega_{q,r}, h) &= \frac{2}{J} \sqrt{\frac{n_B+1}{n_A+1}} \{ f_{1,m}^A(\omega) f_{m,n_A}^A(\omega) [2f_{1,n_B}^B(\omega) \cos(q) + 2f_{1,n_A}^A(\omega) \times \\
&\times ((f_{1,1}^B(\omega))^2 - (f_{1,n_B}^B(\omega))^2)] + ((f_{1,m}^A(\omega))^2 - (f_{m,n_A}^A(\omega))^2) \times \\
&\times (f_{1,1}^B(\omega) + f_{1,1}^A(\omega)) ((f_{1,1}^B(\omega))^2 - (f_{1,n_B}^B(\omega))^2) \}, \quad (47)
\end{aligned}$$

and where $q \equiv Qd$. The local induced magnetization in the subcell B, $\langle S_{j,m}^{B^z} \rangle$, is determined by following the same procedure and by using the function $\ll b_{j,m}; b_{j,m}^\dagger \gg$.

The average induced magnetization in the cell, $\langle S_{cel}^z \rangle$, is defined as

$$\langle S_{cel}^z \rangle = \frac{1}{N(n_A + n_B)} \left[\sum_{l=1}^N \left(\sum_{m=1}^{n_A} \langle S_{l,m}^{A^z} \rangle + \sum_{m=1}^{n_B} \langle S_{l,m}^{B^z} \rangle \right) \right] \quad (48)$$

and from this expression, for the case $h_A = h_B \equiv h$, we obtain susceptibility χ^{zz} , which is given by

$$\chi^{zz} = \frac{d}{dh} \langle S_{cel}^z \rangle. \quad (49)$$

Figure 11 shows the average magnetization in the cell and the susceptibility as a function of h at $T = 0$, for $J = 1$, $J_A = 2$, $J_B = 3$, $h_A = h_B = h$ and $n_A = n_B = 2$. As can be seen, the magnetization presents three plateaus which are limited by four critical fields, h_c , which correspond to the singular points of the susceptibility χ^{zz} ($\chi^{zz} \rightarrow \infty$ when $h \rightarrow h_c$). These four singularities correspond to the modes of zero energy with wave number equal to 0 or π , which limit each energy band. For this case, the critical fields can be obtained exactly from eq. (23) and are given by

$$\begin{aligned}
h_{1c} &= \frac{5 - \sqrt{5}}{4} \cong 0.691, \\
h_{2c} &= \frac{\sqrt{29} - 1}{4} \cong 1.096, \\
h_{3c} &= \frac{\sqrt{29} + 1}{4} \cong 1.596, \\
h_{4c} &= \frac{\sqrt{5} + 5}{4} \cong 1.809.
\end{aligned} \tag{50}$$

It should be noted that the plateaus, where the susceptibility goes to zero, correspond to the gaps in the spectrum.

Figure 12 shows the average induced magnetization, at $T = 0$, for $J = 1$, $J_A = 2$, $J_B = 3$, $h_A = h_B = h$ and $n_A = 2, n_B = 3$, as a function of h . In this case, since the number of sites per cell is odd, there is a zero energy mode even for $h = 0$, and consequently there is no zero magnetization plateaux as in the case shown in Fig. 11. The critical behaviour is, naturally, also present when we have an inhomogeneous field, $h_A = 1.25h_B = h$, and this is shown in Fig. 13 for a larger unit cell, $n_A = 2, n_B = 3$.

In Fig. 14 we present the magnetization for finite temperature ($\beta J = 50$) for the superlattice considered in Fig. 13 with $h_A = h_B = h$. Although the central regions of each plateaux remain, as expected, the thermal fluctuations suppress the quantum transitions.

5 The Two-Spin Correlation Function in the Field Direction

For sites in the subcell A , for example, the two-spin static correlation function in the field direction is defined by

$$\begin{aligned}
\langle S_{j,m}^{A_z} S_{j+r,n}^{A_z} \rangle &= \langle a_{j,m}^\dagger a_{j,n} a_{j+r,m}^\dagger a_{j+r,n} \rangle + \\
&- \frac{1}{2} \left(\langle a_{j,m}^\dagger a_{j,m} \rangle + \langle a_{j,n}^\dagger a_{j,n} \rangle \right) + \frac{1}{4}.
\end{aligned} \tag{51}$$

The average value $\langle a_{j,m}^\dagger a_{j,n} a_{j+r,m}^\dagger a_{j+r,n} \rangle$ can be obtained from the expression

$$\langle a_{j,m}^\dagger a_{j,n} a_{j+r,m}^\dagger a_{j+r,n} \rangle = \frac{1}{\pi} \int_{-\infty}^{\infty} \frac{Im \left(\langle \langle a_{j+r,n}^\dagger a_{j,m}^\dagger a_{j,m} a_{j+r,n} \rangle \rangle \right)}{e^{\beta\omega} + 1} d\omega, \tag{52}$$

where the Fourier transform of the Green function $\ll a_{j+r,n}; a_{j,m}^\dagger a_{j,m} a_{j+r,n}^\dagger \gg$, by using Wick's theorem, can be shown to be written in the form

$$\begin{aligned}
\langle\langle a_{j+r,n}; a_{j,m}^\dagger a_{j,m} a_{j+r,n}^\dagger \rangle\rangle &= \delta_{m,n} \delta_{r,0} \langle\langle a_{j+r,n}; a_{j,m}^\dagger \rangle\rangle + \\
&+ \langle a_{j,m}^\dagger a_{j,m} \rangle \langle\langle a_{j+r,n}; a_{j+r,n}^\dagger \rangle\rangle \\
&- \langle a_{j+r,n}^\dagger a_{j,m} \rangle \langle\langle a_{j+r,n}; a_{j,m}^\dagger \rangle\rangle.
\end{aligned} \tag{53}$$

Then, the correlation function $\langle S_{j,m}^{A^z} S_{j+r,n}^{A^z} \rangle$ can be obtained from the equation

$$\begin{aligned}
\langle S_{j,m}^{A^z} S_{j+r,n}^{A^z} \rangle &= \frac{\delta_{m,n} \delta_{r,0}}{\pi} \int_{-\infty}^{\infty} \frac{Im \langle\langle a_{j+r,n}; a_{j,m}^\dagger \rangle\rangle}{e^{\beta\omega} + 1} d\omega + \\
&- \frac{\langle a_{j+r,n}^\dagger a_{j,m} \rangle}{\pi} \int_{-\infty}^{\infty} \frac{Im \langle\langle a_{j+r,n}; a_{j,m}^\dagger \rangle\rangle}{e^{\beta\omega} + 1} d\omega + \\
&+ \langle a_{j,m}^\dagger a_{j,m} \rangle \langle a_{j+r,n}; a_{j+r,n}^\dagger \rangle + \\
&- \frac{1}{2} \left(\langle a_{j,m}^\dagger a_{j,m} \rangle + \langle a_{j,n}^\dagger a_{j,n} \rangle \right) + \frac{1}{4}.
\end{aligned} \tag{54}$$

The Green function $\ll a_{j+r,n}; a_{j,m}^\dagger \gg$ can be obtained by using eqs. (6), (13) and (18), and is given by [13]

$$\begin{aligned}
\langle\langle a_{j+r,n}; a_{j,m}^\dagger \rangle\rangle &= \frac{2}{NJ} \sqrt{\frac{n_B + 1}{n_A + 1}} \sum_Q \exp(-iqr) \{ f_{m,n}^A(\omega) + \\
&+ \frac{1}{R_Q(\omega)} \{ ((f_{1,n_B}^B(\omega))^2 - (f_{1,1}^B(\omega))^2) \times \\
&\times [f_{m,n_A}^A(\omega) f_{n,n_A}^A(\omega) f_{1,1}^A(\omega) - f_{m,n_A}^A(\omega) f_{1,n}^A(\omega) f_{1,n_A}^A(\omega) + \\
&+ f_{1,m}^A(\omega) f_{1,n}^A(\omega) f_{1,1}^A(\omega) - f_{1,m}^A(\omega) f_{n,n_A}^A(\omega) f_{1,n_A}^A(\omega)] + \\
&+ f_{1,n_B}^B(\omega) [f_{1,n}^A(\omega) f_{m,n_A}^A(\omega) \exp(iq) + f_{n,n_A}^A(\omega) f_{1,m}^A(\omega) \exp(-iq)] + \\
&+ f_{1,1}^B(\omega) [f_{m,n_A}^A(\omega) f_{n,n_A}^A(\omega) + f_{1,m}^A(\omega) f_{1,n}^A(\omega)] \}.
\end{aligned} \tag{55}$$

Therefore, introducing the previous result in eq. (56) and by using eq. (47) we can obtain numerically the direct static correlation function $\langle S_{j,m}^{A^z} S_{j+r,n}^{A^z} \rangle - \langle S_{j,m}^{A^z} \rangle \langle S_{j+r,n}^{A^z} \rangle$, and the results are shown in Figs. 15 and 16.

In Fig. 15 we present the direct static correlation function as a function of r , at $T = 0$, for

two values of the field of the transverse field, $h = 0.693$ and $h = 0.75$, and for $J = 1$, $J_A = 2$, $J_B = 3$, $h_A = h_B = h$ and $n_A = n_B = 2$, which are the same set of parameters of Fig. 12. The values of the critical fields, for this set of parameters, are given in eq. (52) and the first two values are $h_{1c} \cong 0.691$ and $h_{2c} \cong 1.096$. As can be verified in Fig. 15, for these values of the field, the correlation function presents an oscillatory behaviour and its period increases (period $\rightarrow \infty$) as the field approaches a critical value ($h \rightarrow h_c$).

In Fig. 16 it is also presented the direct static correlation function for the same set of lattice parameters of Fig. 15, for $h = 1.091$ and for $h = 1.1$. Although $h = 1.091$, which lies in the region of increasing magnetization (see Fig. 11), and is very close to the critical field $h_{2c} \cong 1.096$, the oscillatory behaviour is still present in the correlation function. On the other hand, when $h = 1.1$, which lies in a plateau of the magnetization (see also Fig. 11), there is no oscillatory behaviour. It means that the period of the oscillation tends to infinity, and this result is still valid for any value of the field in the plateau. This is consistent with the scaling form and the analytical continuation proposed for this correlation function [15], where the correlation length is associated to the oscillation period.

Although the direct correlations $\langle S_{j,m}^{B^z} S_{j+r,n}^{B^z} \rangle - \langle S_{j,m}^{B^z} \rangle \langle S_{j+r,n}^{B^z} \rangle$ and $\langle S_{j,m}^{A^z} S_{j+r,n}^{B^z} \rangle - \langle S_{j,m}^{A^z} \rangle \langle S_{j+r,n}^{B^z} \rangle$ are not presented, they are easily obtained from the shown results and exhibit qualitatively the same behaviour as $\langle S_{j,m}^{A^z} S_{j+r,n}^{A^z} \rangle - \langle S_{j,m}^{A^z} \rangle \langle S_{j+r,n}^{A^z} \rangle$. This is a consequence of the fact that the critical fields are not dependent on the subcell.

6 Conclusions

We have considered the XY ($s = 1/2$) model on the alternating one-dimensional superlattice (closed chain), and an exact solution was obtained by using the Green function method. The excitation spectrum was determined, and explicit expressions were obtained at arbitrary temperature for the internal energy, the specific heat, the magnetization, the susceptibility, and the two-spin static correlation function in the field direction.

The specific heat as a function of temperature, depending on the superlattice parameters, can present a single or a double peak, and we have shown that, at $T = 0$, dC/dT is different from zero provided there is a zero energy mode on the spectrum.

In the $T = 0$ limit, the behaviour of the system was studied as a function of the transverse field, and we have shown that the induced magnetization as a function of the field presents, alternately, regions of plateaus and of variable magnetization. Also in this temperature limit, the susceptibility in the field direction, χ^{zz} , presents singularities which are associated to phase transitions of second kind induced by the field. These critical points are consequence of the presence of zero energy modes with wave number 0 or π . In passing, it should be noted that this critical behavior, as expected, is suppressed at finite temperatures.

These transitions have been treated within the real space renormalization group approach [16], and its critical exponents determined. The critical exponents can be also obtained directly from the exact expression, as shown elsewhere [13].

The two-spin static correlation function in the field direction, as a function of the separation between the spins, presents an oscillating behaviour in the regions where the magnetization is not constant, and the period of oscillations increases as the field approaches the critical value,

and diverges at $h = h_c$. This behaviour confirms that the static correlation function satisfies the analytical extension of the scaling form proposed for the homogeneous case [15].

Finally we would like to point out that the magnetization as a function of the field has qualitatively the same behavior as those experimentally obtained for the NdCu_2 in the low temperature limit, and these results have been obtained recently by Ellerby *et al.* [17] and Loewenhaupt *et al.* [18]. The agreement is more remarkable in the very low temperature limit, since in this limit the structure is analogous to a superlattice. Although this material is described by a Heisenberg type Hamiltonian, this result suggests that the lattice structure is a predominant factor in defining the magnetic properties of the material.

7 References

- [1] J. R. Childress, R. Kergoat, O. Durand, J.M. George, P. Galtier, J. Miltat and A. Shuhl, *J. Magn. & Magn. Mater.* **130** (1994) 13.
- [2] B. V. Reddy, S. N. Khanna, P. Jena, M. R. Press and S. S. Jaswal, *J. Magn. & Magn. Mater.* **130** (1994) 255.
- [3] J. J. Rhyne, M. B. Salomon, C. P. Flynn, R. W. Erwing and J. A. Borchers, *J. Magn. & Magn. Mater.* **129** (1994) 39.
- [4] E. Lieb, T. Schultz and D. C. Mattis, *Ann. Phys.(NY)* **16** (1961) 406.
- [5] J. Stolze, A. Nopert and G. Müller, *Phys. Rev.* **B52** (1995) 4319.
- [6] V. M. Kontorovich and V. M. Tsurkenik, *Sov. Phys. JETP* **26** (1968) 687.
- [7] J. H. H. Perk, H. W. Capel and M. J. Zuilhof, *Physica* **81A** (1975) 319.
- [8] J. H. H. Perk, Th. J. Siskens and H. W. Capel, *Physica* **89A** (1977) 304.
- [9] L. L. Gonçalves and J.P. de Lima, *J. Magn. Magn. Mater.* **140-144** (1995) 1606.
- [10] J. P. de Lima and L.L. Gonçalves, *Mod. Phys. Lett.* **B22** (1996) 1077.
- [11] L. L. Gonçalves, *Theory of Properties of Some One-Dimensional Systems*, (D.Phil. Thesis, University of Oxford, 1977).
- [12] D. N. Zubarev, *Sov. Phys. Usp.* **3** (1960) 320.
- [13] J. P. de Lima, XY-Model in One-Dimension: New Exact Results, (PhD Thesis, Universidade Federal do Ceará, 1997) in portuguese.
- [14] E. R. Smith, *J. Phys.* **C3** (1970) 1419.
- [15] J. P. de Lima and L. L. Gonçalves, *Mod. Phys. Lett.* **B14&15** (1994) 871.
- [16] L. L. Gonçalves and J.P. de Lima, *J. Phys.: Condens. Matter* **9** (1997) 3447.
- [17] M. Ellerby, K. A. McEwen, M. de Podesta, M. Rotter and E. Gratz E., *J. Phys.: Condens. Matter* **7** (1995) 1897.
- [18] M. Loewenhaupt, Th. Reif, P. Svoboda, S. Wagner, M. Wafenschmidt, H. V. Lohneysen, E. Gratz, M. Rotter, B. Lebeck and Th. Haub, *Z. Phys.* **B101** (1996) 499.

8 Acknowledgements

The partial financial support from CNPq and Finep (Brazilian Agencies) is gratefully acknowledged.

9 Figure Captions

Fig. 1- Unit cell of the alternating superlattice.

Fig. 2- Excitation spectrum of the homogeneous lattice for $n_A = 2, n_B = 3, J = J_A = J_B = 1$, and $h_A = h_B = h = 2$.

Fig. 3- Excitation spectrum for $n_A = 2, n_B = 3, J = 1, J_A = 2, J_B = 3$, and $h_A = h_B = 0$.

Fig. 4- Excitation spectrum for $n_A = n_B = 4, J = 1, J_A = 0.3, J_B = 3$, and $h_A = h_B = 0$.

Fig. 5- Internal energy as a function of temperature ($T^* \equiv k_B T$) for $n_A = n_B = 10, J = 1, J_A = 2, J_B = 3$, and $h_A = h_B = 1.5$.

Fig. 6- Specific heat as a function of temperature ($T^* \equiv k_B T$) for $n_A = n_B = 10, J = 1, J_A = 2, J_B = 3$, and $h_A = h_B = 1.5$.

Fig. 7- Specific heat as a function of temperature ($T^* \equiv k_B T$) for $n_A = n_B = 2, J = 1, J_A = 2, J_B = 3$, and $h_A = h_B = 1.3$.

Fig. 8- Specific heat as a function of temperature ($T^* \equiv k_B T$) for $n_A = n_B = 2, J = 1, J_A = 2, J_B = 3$, and $h_A = h_B = 1.75$.

Fig. 9- The low temperature behaviour of the specific heat shown in Fig. 7 ($T^* \equiv k_B T$).

Fig. 10- The low temperature behaviour of the specific heat shown in Fig. 8 ($T^* \equiv k_B T$).

Fig. 11- (a) Average magnetization per subcell A and B (dashed line), and per unit cell (continuous line) as a function of the field, and (b) the susceptibility in the field direction also as a function of the field, for $n_A = n_B = 2, J = 1, J_A = 2, J_B = 3$, and $h_A = h_B = h$, at $T = 0$. The critical fields are $h_{1c} \cong 0.691, h_{2c} \cong 1.096, h_{3c} \cong 1.5960$ and $h_{4c} \cong 1.809$.

Fig. 12- Average magnetization per unit cell as a function of the field, for $n_A = 2, n_B = 3, J = 1, J_A = 2, J_B = 3$, and $h_A = h_B = h$, at $T = 0$.

Fig. 13- Average magnetization per unit cell as a function of the field, for $n_A = n_B = 4, J = 1, J_A = 2, J_B = 3$, and $h_A = 1.25h_B = h$, at $T = 0$.

Fig. 14- Average magnetization per unit cell as a function of the field, for $n_A = n_B = 4, J = 1, J_A = 2, J_B = 3$, and $h_A = h_B = h$, at finite temperature ($\beta J = 50$).

Fig. 15- The direct static correlation function in the field direction, $\rho^{A^z}(r) \equiv \langle S_{j,2}^{A^z} S_{j+r,2}^{A^z} \rangle - \langle S_{j,2}^{A^z} \rangle^2$, as a function of the distance between cells, for $n_A = n_B = 2, J = 1, J_A = 2, J_B = 3$, and $h_A = h_B = h$, at $T = 0$, for $h = 0.75$ (a) and $h = 0.693$ (b).

Fig. 16- The direct static correlation function in the field direction, $\rho^{A^z}(r) \equiv \langle S_{j,2}^{A^z} S_{j+r,2}^{A^z} \rangle - \langle S_{j,2}^{A^z} \rangle^2$, as a function of the distance between cells, for $n_A = n_B = 2, J = 1, J_A = 2, J_B = 3$, and $h_A = h_B = h$, at $T = 0$, for $h = 1.1$ (a) and $h = 1.091$ (b).

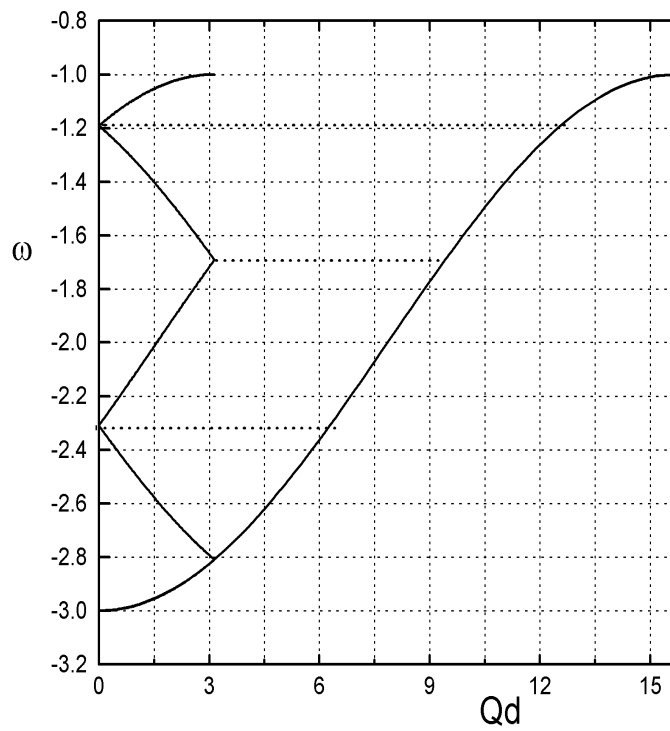
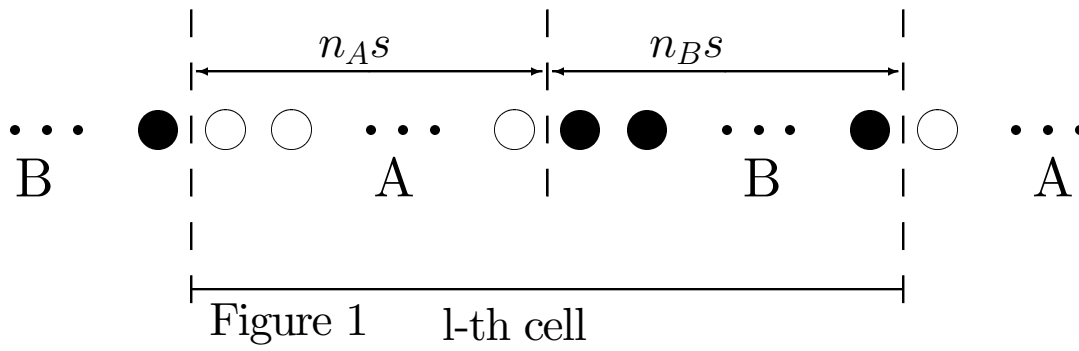


Figure 2

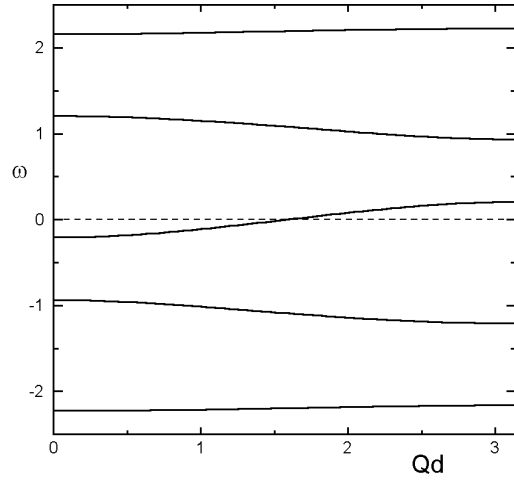


Figure 3

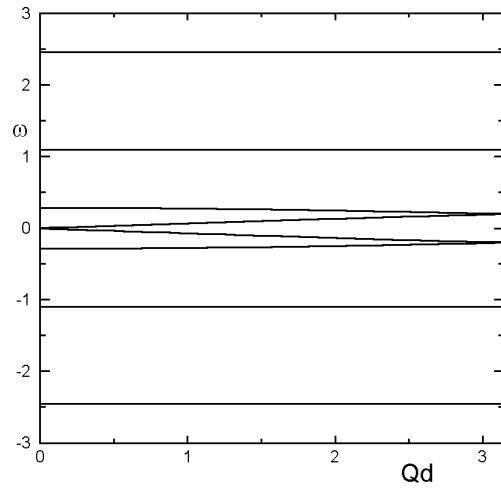


Figure 4

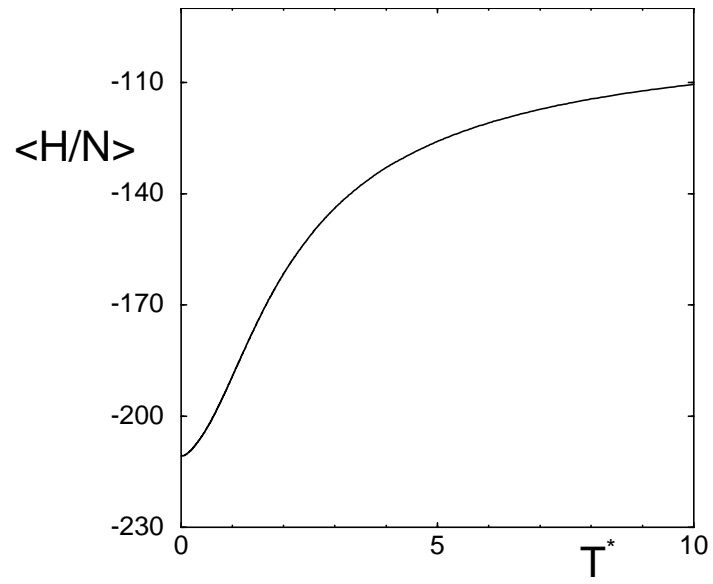


Figure 5

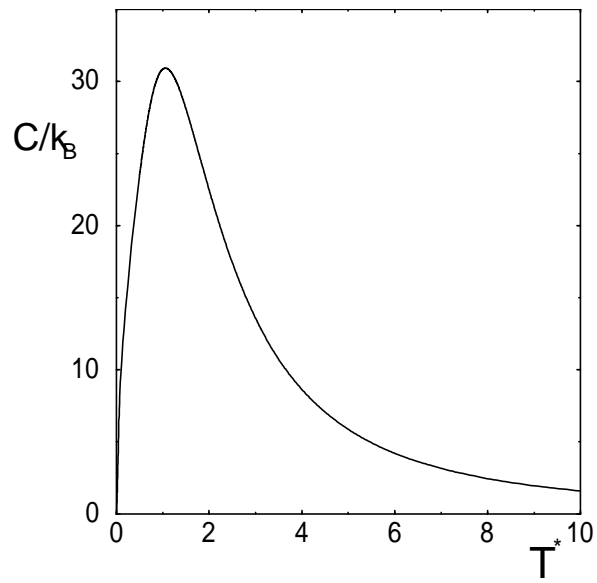


Figure 6

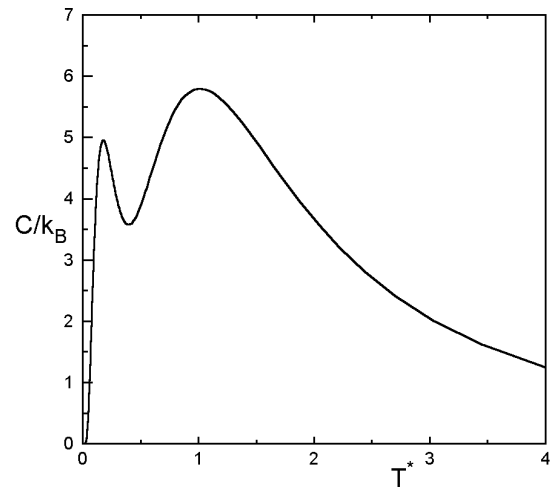


Figure 7

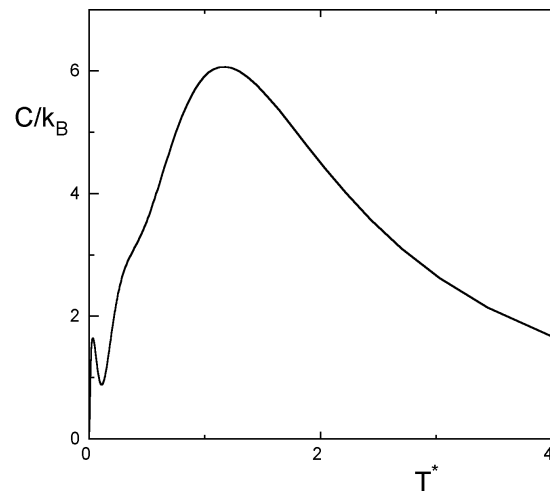


Figure 8

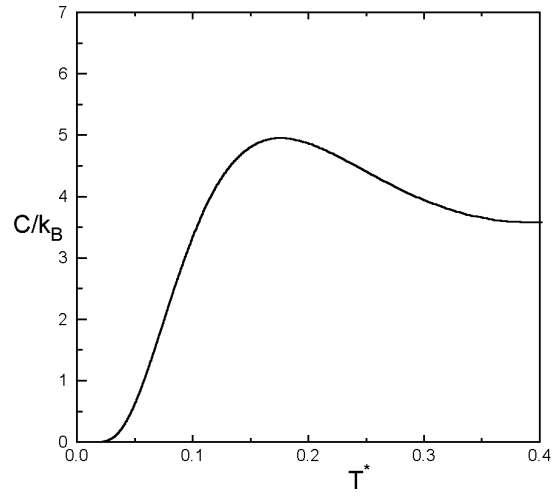


Figure 9

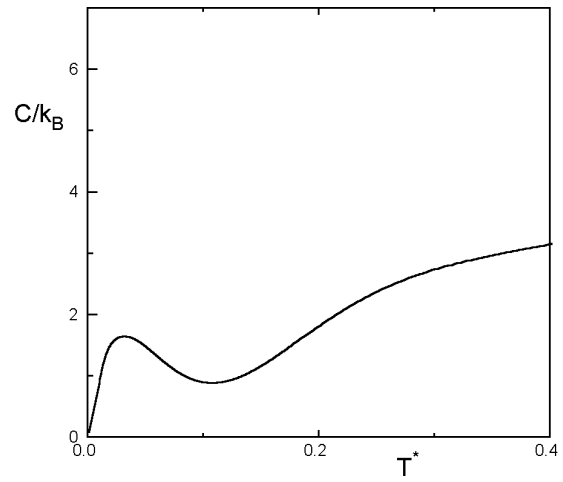


Figure 10

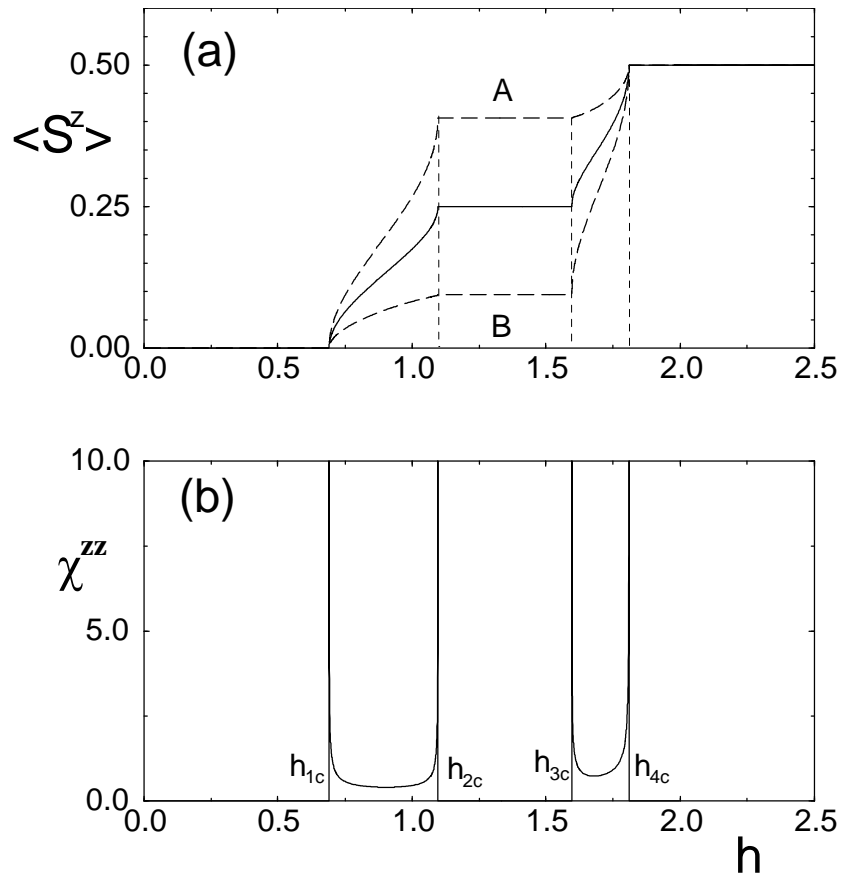


Figure 11

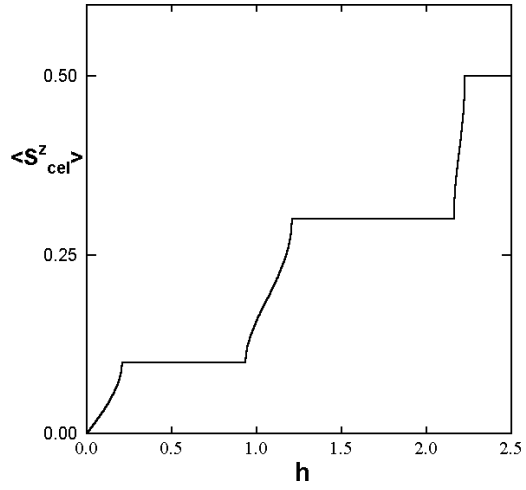


Figure 12

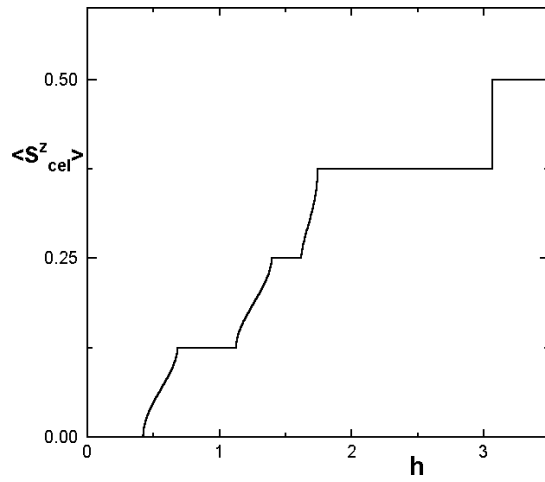


Figure 13

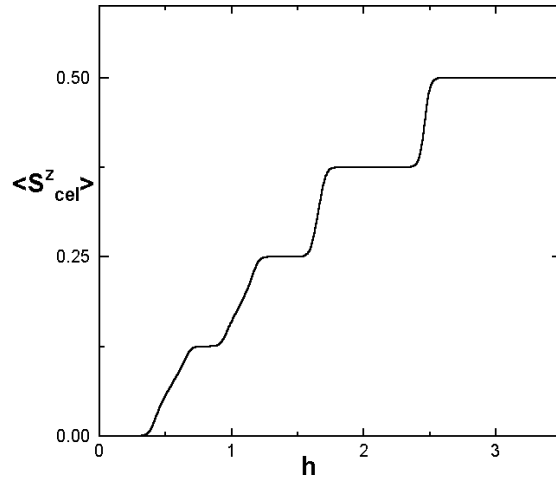


Figure 14

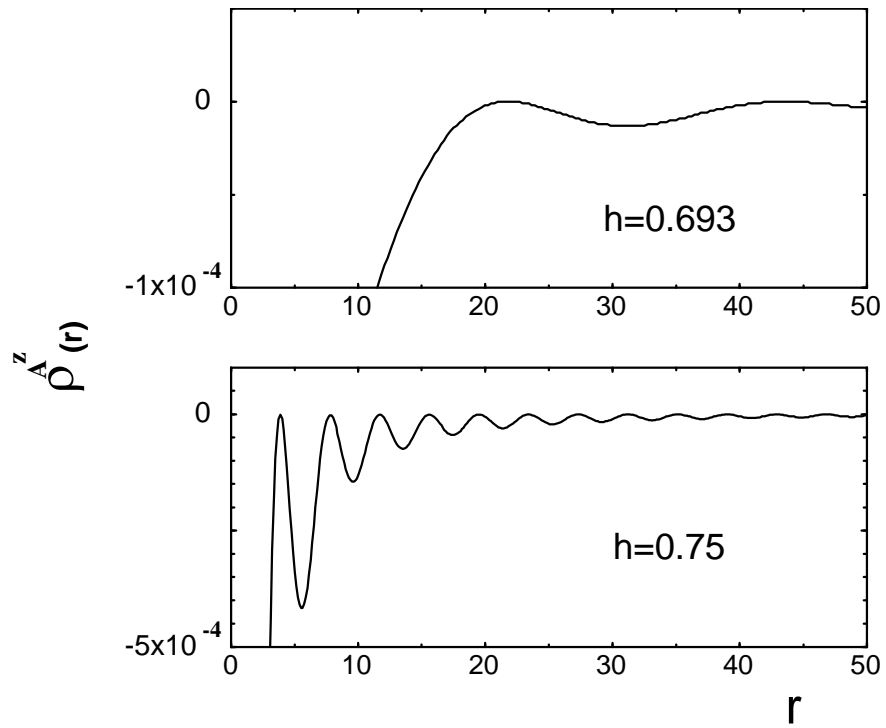


Figure 15

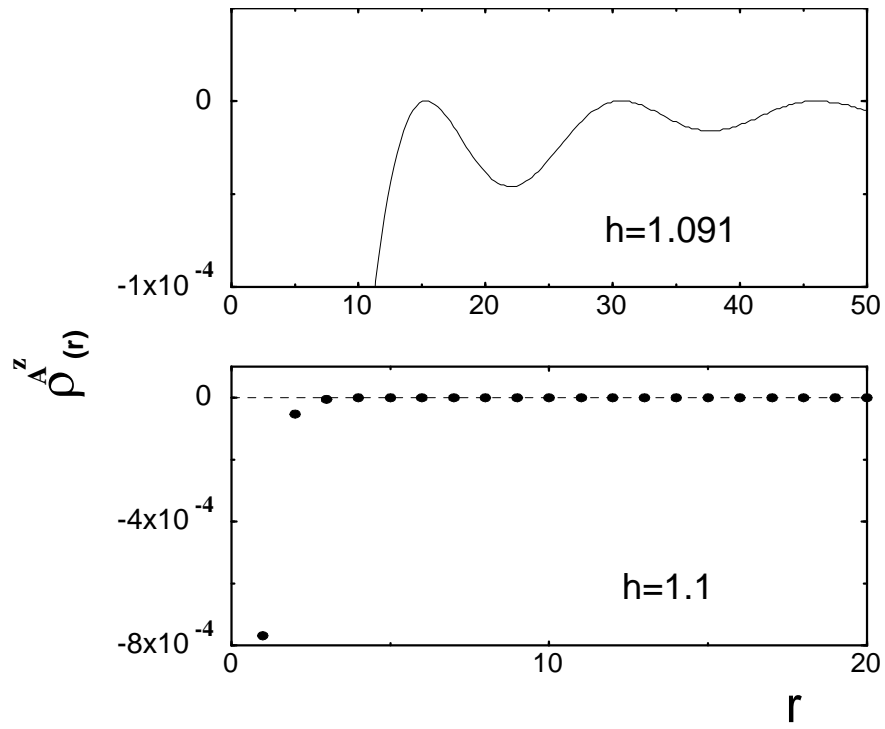


Figure 16